Article

Numerical Simulation of Gas Production from Gas Shale Reservoirs—Influence of Gas Sorption Hysteresis

Jamiu M. Ekundayo * and Reza Rezaee

Discipline of Petroleum Engineering, Western Australian School of Mines: Minerals, Energy and Chemical Engineering, Curtin University, 26 Dick Perry Avenue, Kensington, WA 6151, Australia
* Correspondence: Jamiu.Ekundayo@student.curtin.edu.au

check for updates

Abstract: The true contribution of gas desorption to shale gas production is often overshadowed by the use of adsorption isotherms for desorbed gas calculations on the assumption that both processes are identical under high pressure, high temperature conditions. In this study, three shale samples were used to study the adsorption and desorption isotherms of methane at a temperature of 80 °C, using volumetric method. The resulting isotherms were modeled using the Langmuir model, following the conversion of measured excess amounts to absolute values. All three samples exhibited significant hysteresis between the sorption processes and the desorption isotherms gave lower Langmuir parameters than the corresponding adsorption isotherms. Langmuir volume showed positive correlation with total organic carbon (TOC) content for both sorption processes. A compositional three-dimensional (3D), dual-porosity model was then developed in GEM® (a product of the Computer Modelling Group (CMG) Ltd., Calgary, AB, Canada) to test the effect of the observed hysteresis on shale gas production. For each sample, a base scenario, corresponding to a "no-sorption" case was compared against two other cases; one with adsorption Langmuir parameters (adsorption case) and the other with desorption Langmuir parameters (desorption case). The simulation results showed that while gas production can be significantly under-predicted if gas sorption is not considered, the use of adsorption isotherms in lieu of desorption can lead to over-prediction of gas production performances.

Keywords: organic-rich shale; gas adsorption and desorption; sorption hysteresis; Langmuir model; compositional 3D; dual-porosity system; total organic carbon (TOC); Computer Modelling Group (CMG); GEM®

1. Introduction

Gas production from shale rocks has gained attention worldwide due to advances in hydraulic fracturing and multi-lateral drilling technologies [1,2]. Shale rocks have affinities for gas storage in the internal surface areas of their pore structures, particularly their organic matter pores, and their natural fractures [3,4]. Therefore, gas adsorption and desorption mechanisms must be considered during shale gas reserves evaluations and shale gas production predictions respectively [5–7]. Research has found that gas production can be significantly under-predicted if "adsorption" is not accounted for in the calculation [1,2,8,9]. The word "adsorption" in this context signals a traditional practice of using adsorption isotherms to obtain desorbed gas volumes during gas production calculations [1,2,8,9]. This practice is based on the assumption that both sorption processes follow the reversible monolayer adsorption theory underpinning the Langmuir model [10], which is arguably the standard model for shale gas adsorption isotherms [2,11]. This assumption invariably ignores the hysteresis behavior of shale gas adsorption and desorption isotherms at in situ conditions.

Sorption hysteresis is the term used to describe the difference between adsorption and desorption isotherms for a given adsorbate-adsorbent system. As the pressure is lowered to produce gas, adsorbed gas molecules in the pores and surface of the adsorbent begin to desorb. Where the adsorption process is characterized by capillary condensation, the amount of desorbed gas at a given pressure is often different from the amount initially adsorbed at the same pressure [12–14]. Different hysteresis behavior have been reported, at conditions beyond which capillary condensation can occur, mostly through experimental studies, in methane-coal, carbon dioxide-coal and nitrogen-coal systems [7,15–17]. However, very few literatures exist on shale gas desorption isotherms and by implication, limited resources exist on shale gas sorption hysteresis in spite of the large volume of published work on shale gas adsorption isotherms [7,16,18–20]. While it is not exactly clear why shale gas desorption is not so widely studied like adsorption, despite that it is clearly understood that desorption is akin to shale gas production, it can be speculated that the assumption that the Langmuir isotherm is valid for modeling shale gas sorption processes invariably makes researchers assume that the desorption isotherm should be exactly the same as the adsorption isotherm. Hence, it is the norm to use adsorption isotherm data for desorbed gas volume during shale gas production calculations [1,2,8,9].

Although it is well-acknowledged that gas desorption is one of the multiple complex flow mechanisms characterizing gas production from shale reservoirs [1,2,6,8,11], the true contribution of gas desorption is often masked by the assumption of reversible sorption isotherms. Despite the published results on the contributions of "adsorption" to shale gas production, we are not aware of any literature that explicitly discussed or quantified the amount of gas over-predicted by using adsorption isotherms in lieu of desorption isotherms for gas production predictions. Hence, the main objective of this work is to demonstrate that the existence of sorption hysteresis means different model parameters and consequently, different gas production performances for adsorption and adsorption isotherms. Assuming adsorption equates desorption can result in significant over-prediction of gas production performances.

2. Samples and Methods

2.1. Samples

The samples used in this study are clay-rich shale samples from the Canning Basin in Western Australia. Sample 1 has a total organic carbon (TOC) content of 1.26 wt% and total clay content of 83.49%, sample 2 has a TOC content of 3.20 wt% and total clay content of 74.28%, while sample 3 has a TOC content 2.82 wt% and total clay content of 67.52%. The mineralogical and geochemical properties of the samples are summarized in Tables 1 and 2, respectively.

Table 1. Mineralogical composition of study samples.

Sample ID	Depth (m)	Quartz (%)	K-feldspar (%)	Plagioclase (%)	Kaolinite (%)	Illite/Mica (%)	Chlorite (%)	Calcite (%)	Pyrite (%)
Sample 1	1390	12.42	1.24	1.84	1.54	67.45	14.50	0.25	0.77
Sample 2	1473	17.39	1.78	3.54	7.14	61.27	5.87	0.42	2.59
Sample 3	1478	20.11	2.63	4.21	1.26	56.19	10.07	3.93	1.60

Table 2. Geochemical properties of study samples. TOC: total organic carbon.

Sample ID	TOC (wt%)	S1 (mg/g)	S2 (mg/g)	S3 (mg/g)	T_{max} (°C)	Ro (%)
Sample 1	1.26	0.63	2.43	0.28	454	1.01
Sample 2	3.20	2.12	7.55	0.51	454	1.01
Sample 3	2.82	1.57	4.66	0.43	456	1.05

The parameters S1, S2 and S3 in Table 2 represent the amount of hydrocarbon and non-hydrocarbon compounds liberated during Rock-Eval 6® (a product of Vinci Technologies, France) pyrolysis of the shale samples [21–23]. S1 is the amount of free hydrocarbon released from the kerogen at 300 °C prior to thermal cracking [21–23] and it corresponds to the first peak detected by the flame ionizing detector (FID) in the Rock-Eval 6® equipment [22,23]. S2, the second peak detected by the FID at a temperature, T_{max}, is the amount of hydrocarbon generated from the thermal cracking of the kerogen and heavy hydrocarbons present in the rock samples [21–23]. S3, the third peak picked by the FID, is the volume of carbon dioxide generated from thermal cracking of kerogen at about 390 °C [21–23]. Combined with the TOC content, these parameters are useful in assessing the hydrocarbon-generating potential of a rock sample. They also give insights, through several indices such as the vitrinite reflectance (Ro), hydrogen index, oxygen index and productivity index, into the type and level of thermal maturity of the organic matters present in the rock sample [21–23].

2.2. Measurements and Modeling of Methane Adsorption and Desorption Isotherms

A high-pressure volumetric analyzer (HPVA-II 200®) purchased from Particulate Systems (a division of Micromeritics, Norcross, GA, United States) was used to measure the methane adsorption and desorption capacities of the shale samples at reservoir temperature (80 °C). The equipment measures gas adsorption and desorption isotherms on pulverized samples using volumetric method, and using helium expansion technique for measuring void volumes. It is equipped with a Microsoft Excel®-based software that automatically computes the isotherms using fluid data obtained from refprop® software. Details of the formulae used in calculating the isotherms and the dependence of the isotherms on equation of state have been discussed in our previous studies [18,24]. Thus, based on the findings from those studies, the equation of state by Soave-Benedict-Webb-Rubin (SBWR-EOS) [25] was adopted to calculate the gas compressibility factors for both helium (for free-space volume calculation) and methane in this study.

For each sample, the measured excess ad/desorbed amounts (V_{exc}) were converted to absolute amounts (V_{abs}) using Equation (1) below. The resulting absolute adsorption was then described with Langmuir model (Equation (2)) for application in gas production calculations:

$$V_{exc} = V_{abs}\left(1 - \frac{\rho_{bulk}}{\rho_{ads}}\right) \tag{1}$$

$$V_{abs} = \frac{V_L P}{P + P_L} \tag{2}$$

A constant adsorbed phase density (ρ_{ads}), obtained as the value of the bulk gas density (ρ_{bulk}) at which the measured excess adsorption isotherm is zero [26], was applied for the conversion of excess sorption isotherms to absolute isotherms. At zero excess adsorption, the adsorbed gas is identical to and indistinguishable from the free bulk gas, and as such, the adsorbed phase density at saturation can be taken as the density of the bulk gas at this point [26]. Thus, adsorbed phase density at saturation was achieved, in this study, by plotting the excess adsorption isotherm as a function of bulk gas density and then extrapolating the decreasing linear trend of the excess adsorption isotherm to the bulk gas density axis [26–28].

The parameters, V_L and P_L in Equation (2) represent the Langmuir volume and pressure, respectively, while P represents equilibrium pressure.

2.3. Numerical Simulation of Shale Gas Production

To illustrate the influence of adsorption and desorption on shale gas production, a pure component (100% methane), single-phase, three-dimensional, dual-porosity compositional model was developed in GEM® based on the "Fractured Gas Reservoir with DUALPOR" example dataset (GMFRR006.DAT) provided by the Computer Modelling Group Ltd. [29]. Table 3 contains a list of the key reservoir and well

parameters used for the base case (no-sorption case). For each sample, an adsorption case (where the Langmuir parameters obtained from the adsorption isotherms were used with the assumption of fully reversible sorption isotherms) and a desorption case (where the Langmuir parameters obtained from the desorption isotherm were used) were compared against the no-sorption case. The "ADGMAXC" and "ADGCSTC" keywords in GEM [29] were used to define the Langmuir volume and the reciprocal of Langmuir pressure for the two comparison cases. Langmuir parameters were taken from Table 4. Natural fractures were assumed to be uniformly spaced and run perpendicular to the I- and J-directions through the entire reservoir thickness.

Table 3. Model parameters used for base case (no-sorption case).

Parameter	Value
Reservoir area, ft^2	1378 by 1378
Reservoir thickness, ft	66
Reservoir pressure, psi	2750
Reservoir temperature, °F	176
Initial gas saturation, %	100
Matrix porosity, fraction	0.04
Fracture porosity, fraction	0.001
Matrix permeability, mD	1×10^{-5}
Fracture permeability, mD	0.001
Fracture spacing, ft	26
Number of layers	1
Number of wells	1
Wellbore radius, ft	0.12
Minimum flowing bottom-hole pressure, psi	350
Compressibility factor, psi^{-1}	1×10^{-6}
Rock density, g/cc	2.65
Duration, year	10

**Table 4.** Langmuir parameters for methane adsorption and desorption isotherms.

Sample	Adsorbed Phase Density, Kg/m^3	Adsorption		Desorption	
		V_L, Scf/ton	P_L, Psi	V_L, Scf/ton	P_L, Psi
Sample 1	118	75	379	65	83
Sample 2	105	151	924	104	202
Sample 3	86	105	508	98	195

3. Results and Discussion

3.1. Methane Adsorption and Desorption Isotherms

Figure 1 shows the excess adsorption and desorption isotherms of methane on all three samples. At each pressure, samples 2 and 3 adsorbed higher amounts of methane than sample 1 at approximately the same equilibrium pressure. This is expected given that both samples have higher TOC contents and lower clay contents than sample 1. However, samples 2 and 3 adsorbed approximately equal amounts up to about 500 psi, pressure beyond which the amount adsorbed by sample 2 becomes greater than those of sample 3. This could be due to the counteracting effects of TOC contents and

clay contents. Sample 2 has higher TOC and should have adsorbed more than sample 3, but its higher clay content seems to have counteracted the expected effect than TOC content at pressures up to 500 psi. Additionally, for each sample, the excess adsorbed amounts increased up to a maximum and then decreased slightly afterwards. This is a typical characteristic of the excess adsorption of supercritical fluids on solids [28]. The maximum excess adsorption occurs at a certain pressure where the rate of densities of the adsorbed and free phases is changing at the same rate with pressure [26,28]. Moreover, significant hysteresis can be seen between the adsorption and desorption isotherms for each sample. It is believed that the primary reason for the observed large hysteresis between the sorption isotherms for each sample is the equation of state used in calculating volume changes during the sorption processes [18]. It has been reported that both the size and type of hysteresis between methane adsorption and desorption isotherms are dependent on the applied equation of state [18].
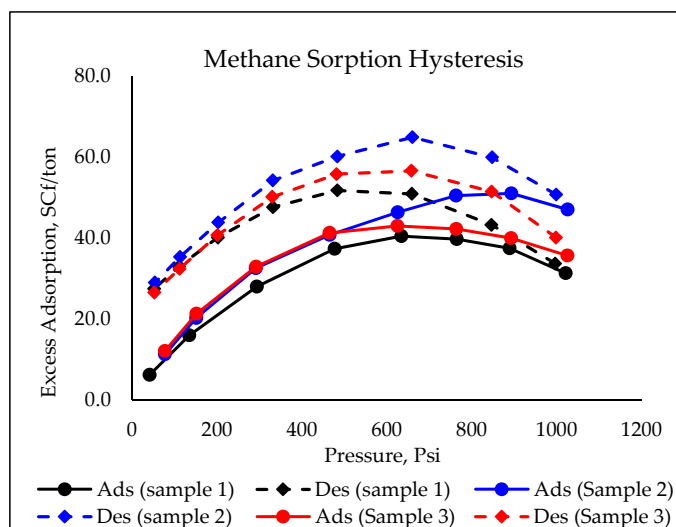
Figure 1. Shale gas adsorption and desorption isotherms measured at 80 °C (176 °F).

Figure 2 shows the excess adsorption isotherm plotted as a function of the bulk gas density for each sample. The dashed lines in the figure indicate the linear "trend-line" fits extrapolated to the bulk-density axis. The density at this point represents the adsorbed phase density at saturation and is equivalent to the ratio of the vertical intercept (of the trend-line) to the slope of the line. While some researchers have argued that this method of estimating the adsorbed phase density can sometimes over-estimate the parameter [30,31], there is no agreement on which method works best. Besides being relatively easier to implement than most of the other known methods, such as the molecular simulation techniques and the adsorbed volume mapping (AVM) method which are generally computationally intensive [32], published data have revealed that the method adopted in this study gives results comparable to other methods such as the three-parameter Langmuir model and Dubinin-Radushkevitch (D-R) equation [30]. While both the three-parameter Langmuir and D-R isotherms have been reported to adequately fit excess adsorption, both have been found to sometimes give unphysical values of the adsorbed phase density [26,30,31]. Moreover, the use of three-parameter Langmuir fit has been reported to be inappropriate at not so high pressures [26], which is the case in this study. As shown in the example (Figure 3) below, while the three-parameter Langmuir model could fit the excess adsorption isotherm, it resulted in low adsorbed phase density leading to high values of Langmuir parameters.
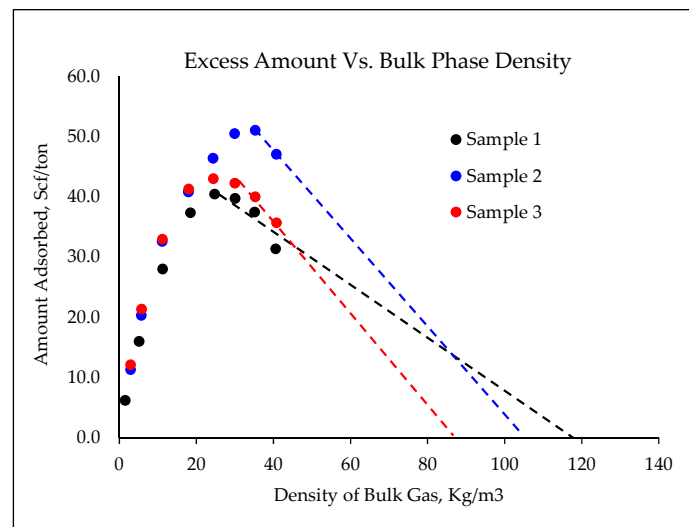
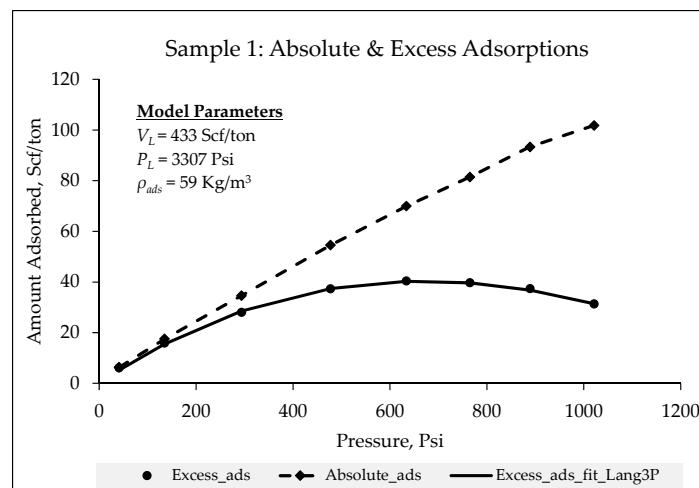**Figure 2.** Estimation of adsorbed phase density.

Figure 3. Example of fitting excess adsorption with three-parameter Langmuir model.

The adsorbed phase density obtained from Figure 2 was used to convert each sample's excess adsorption and desorption isotherms to absolute sorption isotherms using Equation (1). The resulting absolute isotherms were then fitted to Langmuir model (Equation (2)) [10]. Table 4 summarizes the results of the Langmuir fit to the isotherms and the values of the adsorbed phase densities used in converting the isotherms from excess to absolute. For all three sample, Langmuir volumes and pressures obtained from the desorption isotherms are lower than the corresponding values obtained from adsorption isotherms. As shown in Figure 4, the Langmuir volumes for both adsorption and desorption processes correlate positively with TOC content. Such a relationship between Langmuir volume and TOC content has also been reported in the literature [33,34].
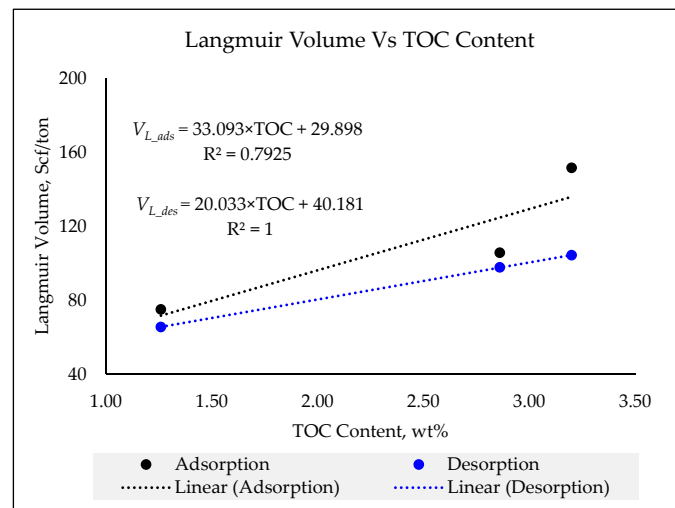
Figure 4. Relationship between Langmuir volumes and TOC content.

3.2. Simulation Results

The results of the numerical simulation with and without sorption parameters are shown in Figure 5 for all three samples. For each sample, the base case gave the lowest gas production rate and 10-year cumulative gas production compared to the other two cases. This confirms the importance of gas sorption parameters on shale gas production calculations. For each sample, the adsorption case gave the highest production rate and cumulative gas production after 10 years resulting in 7%, 18% and 11% additional gas production for samples 1, 2 and 3 respectively (Figure 6). This agrees with existing literatures on the effect of adsorption on shale gas production [1,2,8,9] and also correlates with the TOC contents of the samples. However, the use of adsorption model parameters assumes that the sorption isotherms are fully reversible and no hysteresis exists between them. Such an assumption can lead to a significant over-prediction of gas production depending on the size of the observed hysteresis. Although the desorption case gave higher gas production rate and cumulative gas production than the base case for each sample, its production rate and cumulative gas production are significantly lower than the corresponding values from the adsorption case (Figure 5). The difference between the cumulative gas productions from these two sorption cases was quantified as the effect of sorption hysteresis on gas production. As shown in Figure 6, the assumption of reversible isotherms would result in the over-prediction of the cumulative gas productions, after 10 years, by 5% for each of samples 1 and 3 and by 12% for sample 2.

It follows from the above discussion that while gas sorption generally has a positive effect on gas production from shale reservoirs, the effects are often exaggerated by the assumption of reversible sorption isotherms. Where hysteresis exists between adsorption and desorption isotherms, the (Langmuir) model parameters are usually lower for desorption isotherms than for the adsorption counterparts and the differences will directly translate to lower gas production with the desorption parameters.
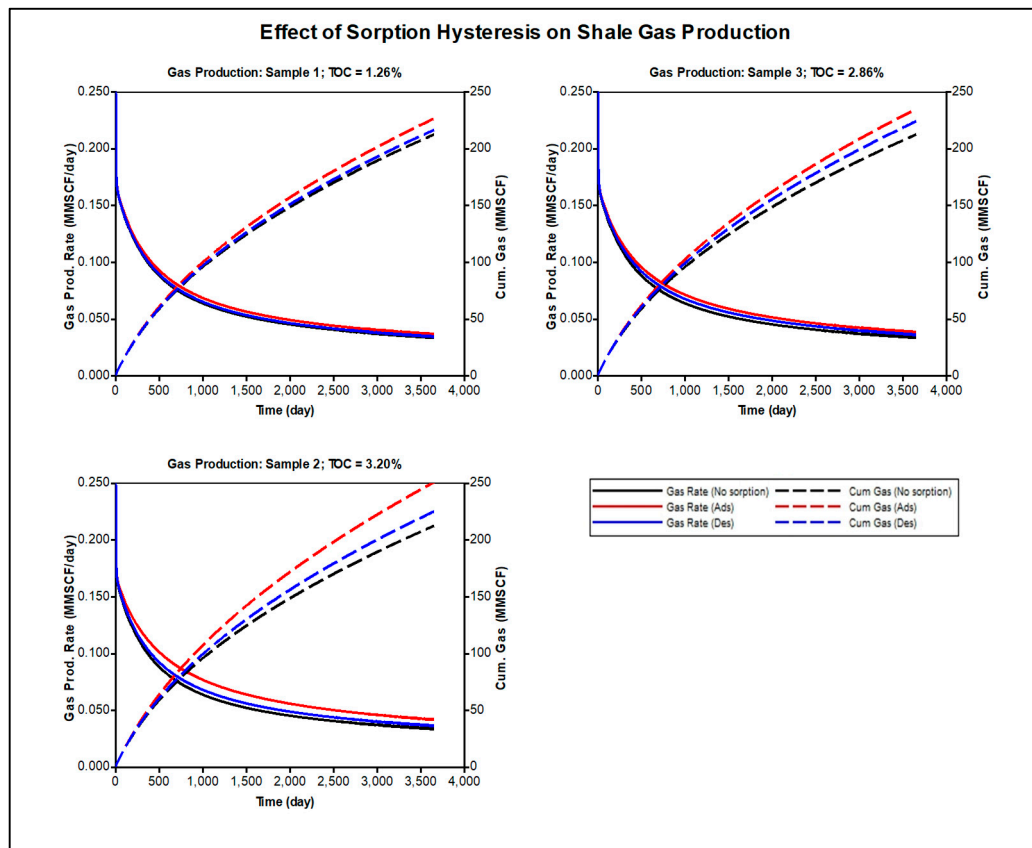
Figure 5. Comparison of shale gas production simulation results.
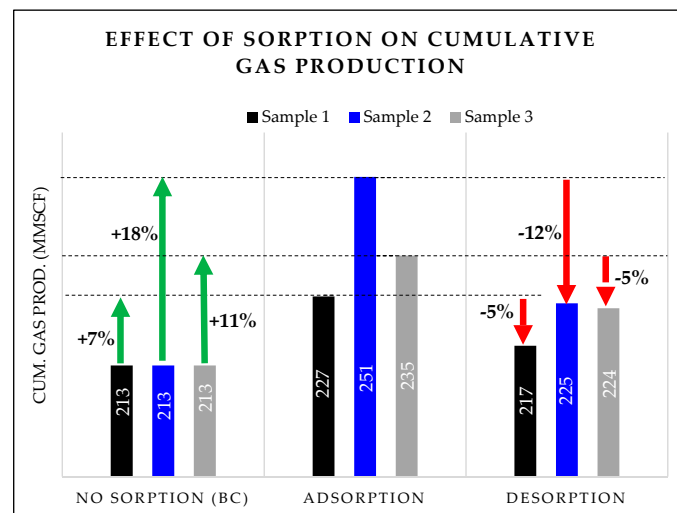

Figure 6. Summary of effects of adsorption and sorption hysteresis on cumulative gas production.

4. Study Limitations

While this study offers insights into the effect of sorption hysteresis on gas production, the following limitations are acknowledged:

1. First, this study included a limited number of samples, which, although revealed the expected trend between Langmuir volume (and hence, gas production) and TOC content, may be too small to make adequate statistical correlation of gas production with TOC content. However, given the positive relationships observed between Langmuir volume and TOC contents (Figure 4)

as well as the positive correlation reported between gas production and Langmuir volume [9], it is envisaged that the findings reported in this study, will be valid irrespective of the number of samples.

2. Additionally, the method employed in this study to calculate the adsorbed phase density uses a linear equation to fit the last few data points, following the maximum excess adsorption, of each isotherm. Thus, the value of the adsorbed phase density obtained depends on the linearity of these data points. For example, as shown in Figure A1 (Appendix A), if the last data point is included for sample 1 the resulting adsorbed phase density becomes lower than the value reported in Table 4. With this lower adsorbed phase density, the calculated Langmuir parameters become higher than they currently are and so are the cumulative gas productions for the two comparison cases. However, these values are still lower than the corresponding values for samples 2 and 3 and as such, the observed trend with TOC content remains unchanged.

3. Finally, the results of the numerical simulation presented in this study are focused only on the effects of sorption processes. In reality, shale gas transport is a multiphysics process and the inclusion of other flow mechanisms may affect the simulation outputs. However, in keeping with the objectives of this study, it was necessary to keep other parameters constant to isolate the effect of sorption parameters and hysteresis on gas production. Several publications exist that adopted similar approach in their studies [1,2,8,9].

5. Conclusions

This study presented the effect of gas adsorption and sorption hysteresis on shale gas production. The results showed that gas desorption might not necessarily follow the same path as gas adsorption, and the sorption isotherms may exhibit significant hysteresis. In such a case, desorption model parameters are much lower than the corresponding adsorption model parameters. Consequently, using adsorption model parameters to calculate desorbed gas volumes during gas production could lead to significant over-prediction of gas production performances. In summary, it can be concluded that:

1. Significant hysteresis was observed between adsorption and desorption isotherms of methane on all three samples under high-pressure, high-temperature conditions.
2. The desorption isotherms gave lower Langmuir parameters compared to the adsorption counterparts.
3. Langmuir volumes for both adsorption and desorption processes showed positive correlation with TOC content.
4. Sorption has a significant positive influence on gas production and as such, neglecting the gas sorption during gas production predictions can lead to under-estimation of gas production performances.
5. The additional gas production due to gas sorption consideration in the gas production calculations increased with TOC content. This is expected given the positive correlation between Langmuir volumes and TOC contents.
6. The use of adsorption Langmuir parameters during gas production calculations can lead to over-prediction of the gas production performances.

Conflicts of Interest: The authors declare no conflict of interest.

Appendix A

Figure A1 below illustrates one of the limitations of this study, which is about the method used to determine the adsorbed phase densities for conversion of excess adsorption to absolute amounts.
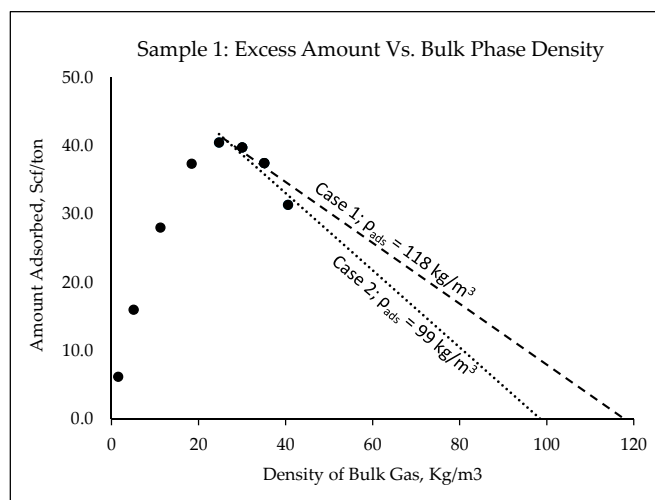
Figure A1. Possible uncertainty in adsorbed phase density determined from excess adsorption versus bulk density plot.

The different between the two cases in the figure lies in the inclusion (or otherwise) of the last data point in the linear fitting of the excess adsorption—bulk density plot post saturation. The Langmuir parameters obtained from these two cases are different, with the case 2 resulting in higher Langmuir parameters than case 1 as shown in Table A1 below:

Table A1. Variations in Langmuir parameters and cumulative gas production between cases 1 and 2.

Case ID	Adsorption			Desorption		
	V_L Scf/ton	P_L Psi	Cum Gas Prod MMScf	V_L Scf/ton	P_L Psi	Cum Gas Prod MMScf
Case 1	75	379	227	65	83	217
Case 2	87	462	231	72	101	218

The 10-year cumulative gas productions obtained from case 2 is higher than case 1 due to its higher Langmuir volumes for both sorption processes. However, these values are still lower than the cumulative gas productions for the other two samples, which is consistent with our conclusions.

References

1. Yu, W.; Huang, S.; Wu, K.; Sepehrnoori, K. Development of A Semi-Analytical Model for Simulation of Gas Production in Shale Gas Reservoirs. In Proceedings of the Unconventional Resources Technology Conference, Society of Exploration Geophysicists, American Association of Petroleum Geologists, Society of Petroleum Engineers, Denver, CO, USA, 25–27 August 2014; pp. 2187–2204.
2. Feast, G.; Wu, K.; Walton, J.; Cheng, Z.F.; Chen, B. Modeling and Simulation of Natural Gas Production from Unconventional Shale Reservoirs. *Int. J. Clean Coal Energy* **2015**, *4*, 23–32. [CrossRef]
3. Curtis, J.B. Fractured shale-gas systems. *AAPG Bull.* **2002**, *86*, 1921–1938.
4. Leahy-Dios, A.; Das, M.; Agarwal, A.; Kaminsky, R.D. Modeling of Transport Phenomena and Multicomponent Sorption for Shale Gas and Coalbed Methane in an Unstructured Grid Simulator. In Proceedings of the SPE ATCE, Denver, CO, USA, 30 October–2 November 2011; pp. 1–9.

5. Wang, J.; Dong, M.; Yang, Z.; Gong, H.; Li, Y. Investigation of Methane Desorption and Its Effect on the Gas Production Process from Shale: Experimental and Mathematical Study. *Energy Fuels* **2016**, *31*, 205–216. [CrossRef]

6. Wang, J.; Luo, H.; Liu, H.; Cao, F.; Li, Z.; Sepehrnoori, K. An Integrative Model To Simulate Gas Transport and Production Coupled With Gas Adsorption, Non-Darcy Flow, Surface Diffusion, and Stress Dependence in Organic-Shale Reservoirs. *SPE J.* **2015**, *22*, 244–264. [CrossRef]

7. Wei, G.; Xiong, W.; Gao, S.; Hu, Z.; Liu, H.; Yu, R. Impact of temperature on the isothermal adsorption/desorption characteristics of shale gas. *Pet. Explor. Dev.* **2013**, *40*, 514–519.

8. Wang, W.; Yu, W.; Hu, X.; Liu, H.; Chen, Y.; Wu, K.; Wu, B. A semianalytical model for simulating real gas transport in nanopores and complex fractures of shale gas reservoirs. *AICHE J.* **2018**, *64*, 326–337. [CrossRef]

9. Zhang, W.; Xu, J.; Jiang, R. Production forecast of fractured shale gas reservoir considering multi-scale gas flow. *J. Pet. Explor. Prod. Technol.* **2017**, *7*, 1071–1083. [CrossRef]

10. Langmuir, I. The adsorption of gases on plane surfaces of glass, mica and platinum. *J. Am. Chem. Soc.* **1918**, *40*, 1361–1403. [CrossRef]

11. Yu, W.; Sepehmoori, K.; Patzek, T.W. Evaluation of Gas Adsorption in Marcellus Shale. In Proceedings of the SPE ATCE, Amsterdam, The Netherlands, 27–29 October 2014; pp. 1–16.

12. Rajniak, P.; Yang, R.T. A Simple Model and Experiments for Adsorption-Desorption Hysteresis: Water Vapor on Silica Gel. *AICHE J.* **1993**, *39*, 774–786. [CrossRef]

13. Kierlik, E.; Monson, P.A.; Rosinberg, M.L.; Tarjus, G. Adsorption hysteresis and capillary condensation in disordered porous solids: A density functional study. *J. Phys. Condens. Matter* **2002**, *14*, 9295–9315. [CrossRef]

14. Monson, G. A model of adsorption-desorption hysteresis in which hysteresis is primarily developed by the interconnections ina network of pores. *Proc. R. Soc. Lond. Ser. A Math. Phys. Sci.* **1983**, *390*, 47–72.

15. Bell, G.J.; Rakop, K.C. Hysteresis of Methane/Coal Sorption Isotherms. In Proceedings of the 61st SPE-ATCE, New Orleans, LA, USA, 5–8 October 1986.

16. Wei, G.; Hu, Z.; Zhang, X.; Yu, R.; Wang, L. Shale Gas Adsorption and Desorption Characteristics and its Effects on Shale Permeability. *Energy Explor. Exploit.* **2017**, *35*, 463–481.

17. Zhang, R.; Liu, S. Experimental and theoretical characterization of methane and CO_2 sorption hysteresis in coals based on Langmiur desorption. *Int. J. Coal Geol.* **2016**, *171*, 49–60. [CrossRef]

18. Ekundayo, M.J.; Rezaee, R. Volumetric Measurements of Methane-Coal Adsorption and Desorption Isotherms—Effects of Equations of State and Implication for Initial Gas Reserves. *Energies* **2019**, *12*, 2022. [CrossRef]

19. Bhowmik, S.; Dutta, P. A study on the effect of gas shale composition and pore structure on methane sorption. *J. Nat. Gas Sci. Eng.* **2019**, *62*, 144–156. [CrossRef]

20. Zhang, Y.; Xing, W.; Liu, S.; Liu, Y.; Yang, M.; Zhao, J.; Song, Y. Pure methane, carbon dioxide, and nitrogen adsorption on anthracite from China over a wide range of pressures and temperatures: Experiments and modeling. *RSC Adv.* **2015**, *5*, 52612–52623. [CrossRef]

21. El Nady, M.M.; Ramadan, F.S.; Hammad, M.M.; Lotfy, N.M. Evaluation of organic matters, hydrocarbon potential and thermal maturity of source rocks based on geochemical and statistical methods: Case study of source rocks in Ras Gharib oilfield, central Gulf of Suez, Egypt. *Egypt. J. Pet.* **2015**, *24*, 203–211. [CrossRef]

22. Peters, K.E. Guidelines for Evaluating Petroleum Source Rock Using Programmed Pyrolysis. In *American Chemical Society, Symposium on Organic Geochemistry of Humic Substances, Kerogen and Coal*; American Association of Petroleum Geologists: Philadelphia, PA, USA, 1985.

23. Lafarge, E.; Marquis, F.; Pillot, D. Tock-Eval 6 Applications in Hydrocarbon Exploration, Production, and Soil Contamination Studies. *Rev. De L'institut Français Du Pétrole* **1998**, *53*, 421–437.

24. Ekundayo, J.; Rezaee, R. Effect of Equation of States on High Pressure Volumetric Measurements of Methane-Coal Sorption Isotherms—Part 1: Volumes of Free Space and Methane Adsorption Isotherms. *Energy Fuels* **2019**, *33*, 1029–1036. [CrossRef]

25. Soave, G.S. An effective modification of the Benedict-Webb-Rubin equation of state. *Fluid Phase Equilibria* **1999**, *164*, 157–172. [CrossRef]

26. Zhang, J.; Clennell, M.B.; Liu, K.; Pervukhina, M.; Chen, G.; Dewhurst, D.N. Methane and Carbon Dioxide Adsorption on Illite. *Energy Fuels* **2016**, *30*, 10643–10652. [CrossRef]

27. Moellmer, J.; Moeller, A.; Dreisbach, F.; Glaeser, R.; Staudt, R. High pressure adsorption of hydrogen, nitrogen, carbon dioxide and methane on the metal–organic framework HKUST-1. *Microporous Mesoporous Mater.* **2011**, *138*, 140–148. [CrossRef]

28. Do, D.D.; Do, H.D. Adsorption of argon from sub- to supercritical conditions on graphitized thermal carbon black and in graphitic slit pores: A grand canonical Monte Carlo simulation study. *J. Chem. Phys.* **2005**, *123*, 084701. [CrossRef] [PubMed]

29. Computer Modelling Group. *GEM Compositional & Unconventional Reservoir Simulator*; USER GUIDE C.M.G. Ltd.: Calgary, AB, Canada, 2016.

30. Zhou, S.; Xue, H.; Ning, Y.; Guo, W.; Zhang, Q. Experimental study of supercritical methane adsorption in Longmaxi shale: Insights into the density of adsorbed methane. *Fuel* **2018**, *211*, 140–148. [CrossRef]

31. Tian, Y.; Yan, C.; Jin, Z. Characterization of Methane Excess and Absolute Adsorption in Various Clay Nanopores from Molecular Simulation. *Sci. Rep.* **2017**, *7*, 12040. [CrossRef] [PubMed]

32. Murata, K.; El-Merraoui, M.; Kaneko, K. A new determination method of absolute adsorption isotherm of supercritical gases under high pressure with a special relevance to density-functional theory study. *J. Chem. Phys.* **2001**, *114*, 4196–4205. [CrossRef]

33. Gasparik, M.; Bertier, P.; Gensterblum, Y.; Ghanizadeh, A.; Krooss, B.M.; Littke, R. Geological controls on the methane storage capacity in organic-rich shales. *Int. J. Coal Geol.* **2014**, *123*, 34–51. [CrossRef]

34. Zou, J.; Rezaee, R.; Liu, K. Effect of Temperature on Methane Adsorption in Shale Gas Reservoirs. *Energy Fuels* **2017**, *31*, 12081–12092. [CrossRef]